

Catalyzed Activation of CO₂ by a Lewis Base Site in W-Cu-BTC Hybrid Metal Organic Frameworks

Qiuju Zhang¹, Lujie Cao¹, Baihai Li^{1,2}, Liang Chen^{1*}

¹Ningbo Institute of Materials Technology and Engineering, Chinese Academy of Sciences, Ningbo, Zhejiang 315201, P. R. China

²Department of Materials Science and Engineering, University of Michigan, Ann Arbor, MI

* Corresponding Author; chenliang@nimte.ac.cn; Fax:+86-574-86685043

List of Contents:

Figure S1. The periodic and cluster models of W-Cu-BTC.

Figure S2. The binding energies (E_{ads}) and adsorbed geometries of CO₂ binding on Mo-Cu-BTC and Cr-Cu-BTC; and HOMO comparison of M-Cu-BTC (M=W, Mo and Cr).

Figure S3. The vibrational modes of CO₂-adsorbed complexes except for η²(CO).

Figure S4. The local density of states (LDOS) of W-Cu-BTC and η²(CO).

Figure S5. The binding energies and geometries of CO₂ binding on W-BTC and Cu-BTC.

Table S1. Comparison of the adsorption energy (E_{ads}) and geometries of CO₂ adsorbed on W-Cu-BTC, Cu-BTC and W-BTC.

Figure S6. The desorption process of formic acid on W-Cu-BTC.

Figure S7. The desorption process of methylene glycol on W-Cu-BTC.

Figure S1. The periodic (a) and cluster (b) models of W-Cu-BTC. The blue, green, red, grey and white balls represent W, Cu, O, C and H atoms, respectively.

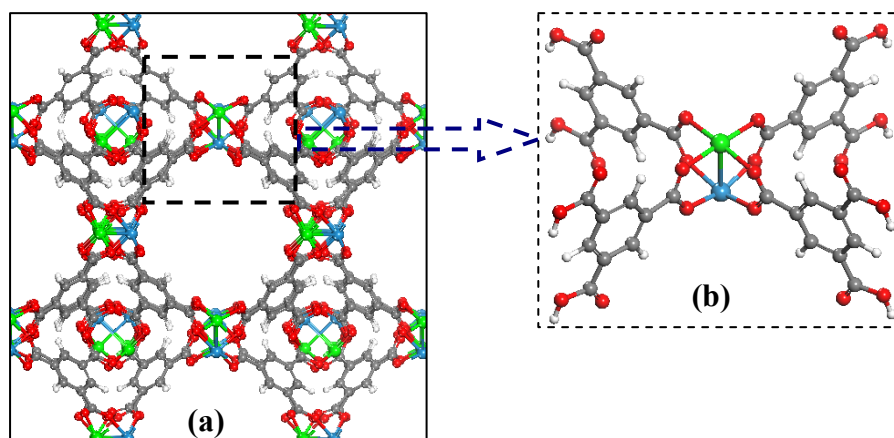


Figure S2. (Top) The binding energies/adsorption energies (E_{ads}) and the adsorbed geometries of CO_2 binding on Mo-Cu-BTC and Cr-Cu-BTC. The abilities of catalyzing CO_2 by the three hybrid MOFs are found to be in the order of $\text{W-Cu-BTC} > \text{Mo-Cu-BTC} > \text{Cr-Cu-BTC}$. Although the coordination complex $\eta^2(\text{CO})$ can be formed on Mo-Cu-BTC, the binding energy of 0.44 eV is much smaller than that of W-Cu-BTC (1.34 eV). In the case of Cr-Cu-BTC, the $\eta^2(\text{CO})$ complex can not be obtained. Instead, the structural optimization shows a favorable angularly-binding structure ($\eta^1_2(\text{O})$) with CO_2 remaining the original linear structure ($E_{\text{ads}} = 0.33$ eV), which indicates that the Cr-Cu node is unable to activate CO_2 . Indeed, as mentioned in the introduction, the ability to activate CO_2 is related to the ability of losing electrons, which is in the order of $\text{Cr} < \text{Mo} < \text{W}$.

(Bottom) The comparison of HOMO for W-Cu-BTC, Mo-Cu-BTC and Cr-Cu-BTC. The gradually weaker $d\pi^2$ character is well consistent with the weaker catalyzing ability in the order of $\text{W-Cu-BTC} > \text{Mo-Cu-BTC} > \text{Cr-Cu-BTC}$.

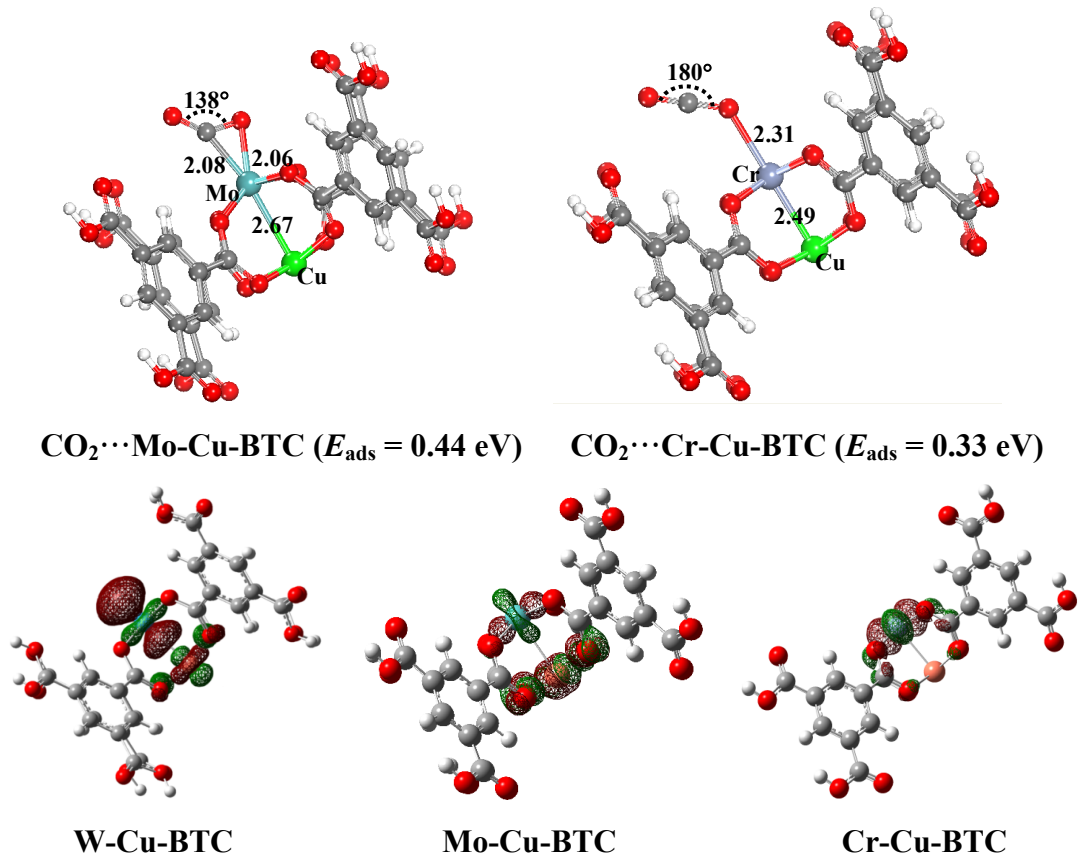
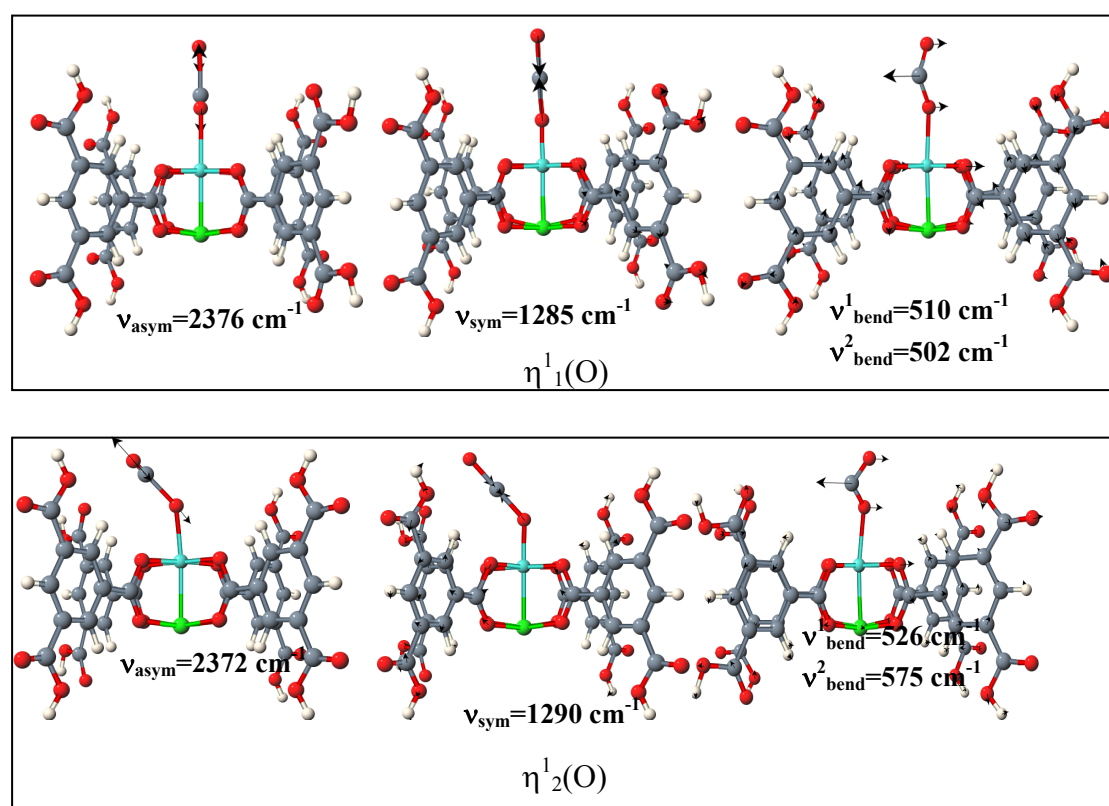


Figure S3. The vibrational frequency modes of CO₂ adsorption on the open metal W sites in various models except $\eta^2(\text{CO})$.



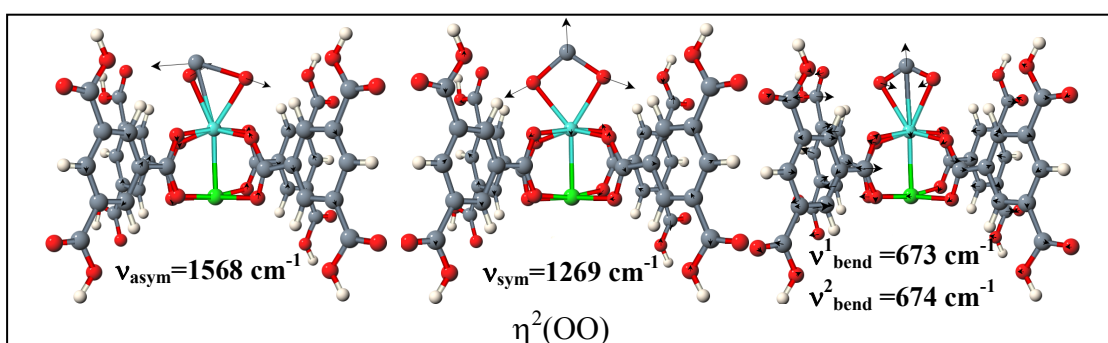
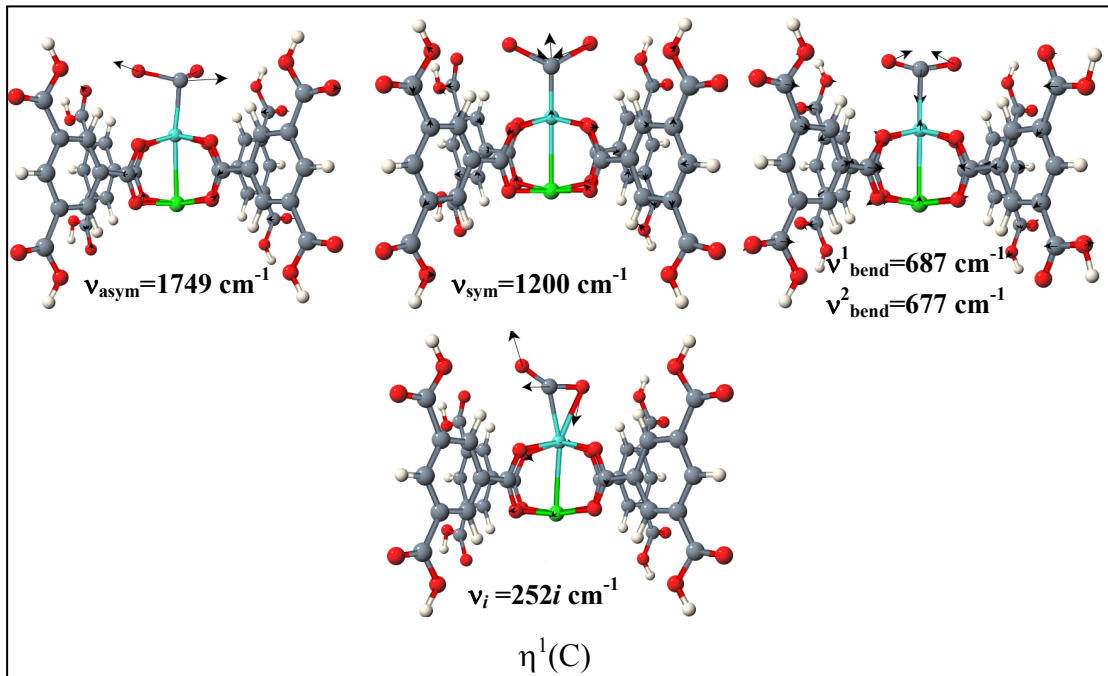


Figure S4. LDOS of the open W ion in W-Cu-BTC and $\eta^2(\text{CO})$ complex of $\text{CO}_2\text{-W-Cu-BTC}$ including the $6s$, $5d_{z^2}$ and the $5d$ orbitals.

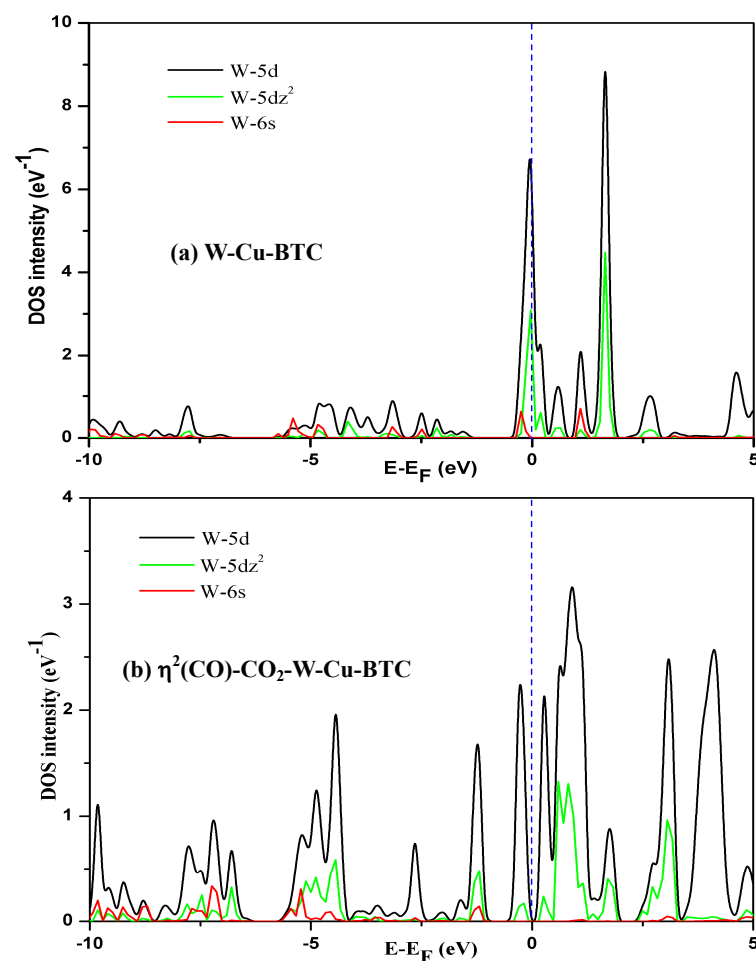


Figure S5. The physisorbed structures and binding energies/adsorption energies (E_{ads}) of CO₂ angularly and linearly binding on W-BTC (top layer) and Cu-BTC (bottom layer).

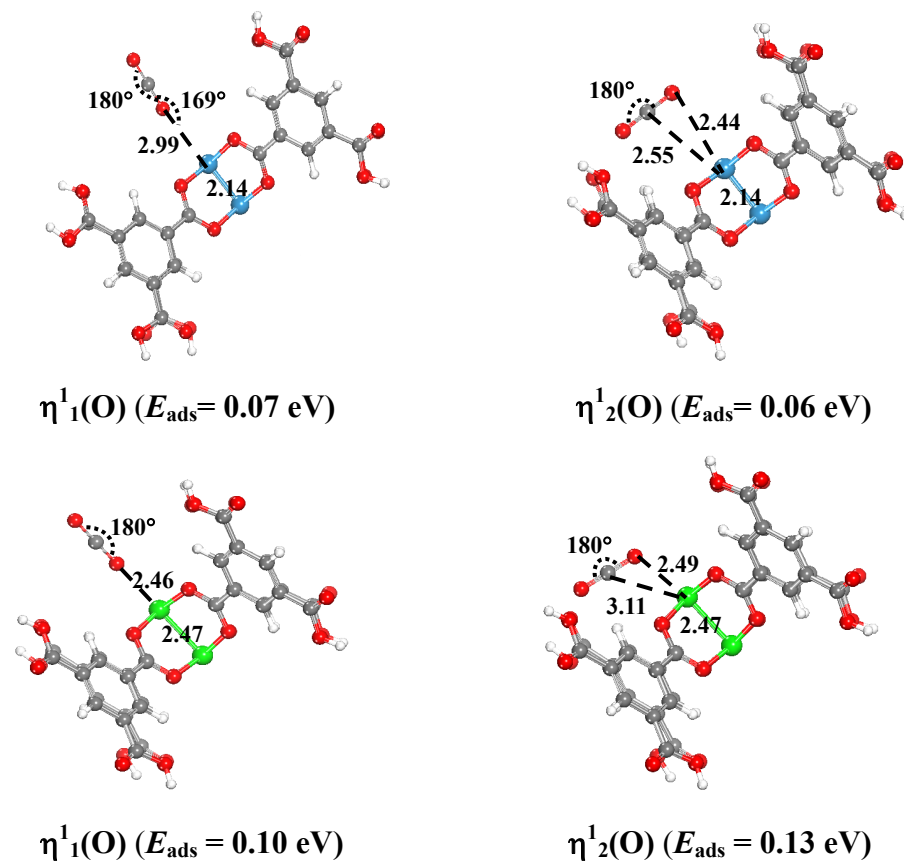


Table S1. Comparison of the adsorption energy (E_{ads}) and geometries of CO₂ adsorbed on W-Cu-BTC, Cu-BTC and W-BTC.

	W-Cu-BTC		Cu-BTC		W-BTC	
	E_{ads}	$\angle \text{COC}$	E_{ads}	$\angle \text{COC}$	E_{ads}	$\angle \text{COC}$
$\eta^1_1(\text{O})$	0.22	180°	0.10	180°	0.07	180°
$\eta^1_2(\text{O})$	0.24	178°	0.13	180°	0.06	180°
$\eta^1(\text{C})$	0.25	144°	-	-	-	-
$\eta^2(\text{CO})$	1.34	136°	-	-	-	-
$\eta^2(\text{OO})$	-0.40	108°	-	-	-	-

Figure S6. The desorption process of formic acid (HCOOH) from W-Cu-BTC after hydrogenation by two H atoms on the activated CO₂ in η²(CO) complex.

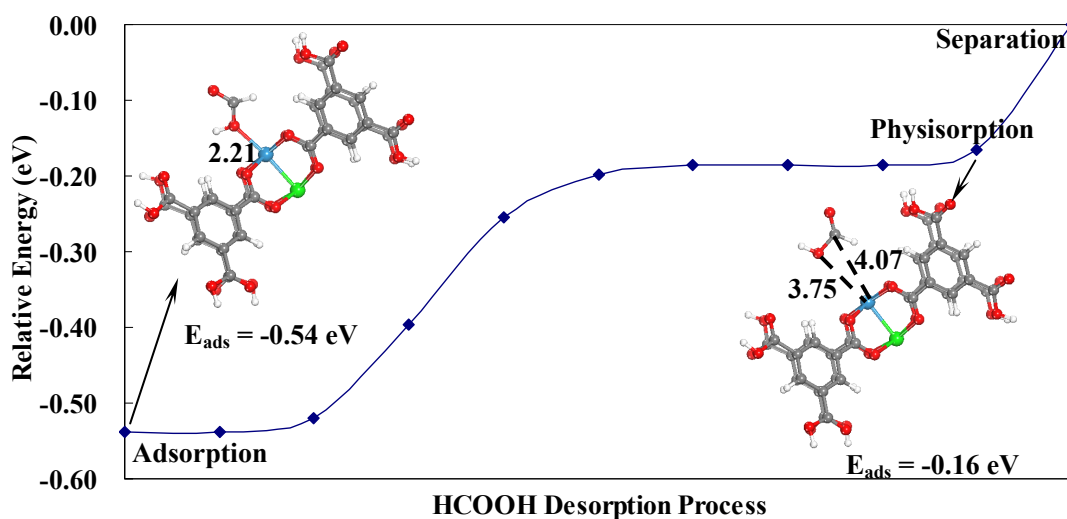


Figure S7. The desorption process of methylene glycol (H₂C(OH)₂) from W-Cu-BTC after hydrogenation by four H atoms on the activated CO₂ in η²(CO) complex.

